euspen's 20th International Conference & Exhibition, Geneva, CH, June 2020
www.euspen.eu

Compression effects of epoxy coating in microcutting of calcium fluoride single crystals

Yan Jin Lee* and Rou Ting Tan

Department of Mechanical Engineering, National University of Singapore, 9 Engineering Drive 1, Singapore 117575, Singapore

**lionel.lyj@u.nus.edu*

Abstract
In this age where high precision technology thrives in micro-optical applications, the augmentation of manufacturing productivity has never been more needful. Optical-grade surfaces can be difficult to machine on brittle materials that limit the critical depth of cut, requiring multi-step precision machining tool paths to achieve the desired surfaces by conventional means. Despite multiple advances in improving ultraprecision machining technology, these developments involve sophisticated equipment with precision control to achieve material removal capabilities with high accuracies. Therefore, a novel technique is visited to enhance ductile-mode machining of microfeatures on single crystal calcium fluoride optics by single point diamond machining with a solidified coating. This paper confirms the mechanical influence of the coating as observed by the anisotropic improvements in the ductile–brittle transition (DBT) on the (100)-plane oriented crystal with the application of varying two-part type epoxy coating thicknesses (2–10 µm). The strong influence of the coating thickness on the enhancement of ductile-mode machining is subsequently investigated along the $(111)[0\bar{1}1]$ direction, with an average enhancement factor of 2.57. An analytical analysis of the work material stress status during microcutting with the coating indicates high compressive stresses and an increase in shear strength of the material.

Keywords: epoxy coating, ductile-mode cutting, calcium fluoride, ultraprecision machining, surface effect

1. Introduction

Calcium fluoride (CaF_2) single crystal is a promising material that is used in optical windows applications such as spectrometers, lithography, microfluidic channels, and micro-resonators. The popularity of the material is a result of its excellent optical properties such as a wide transmission range from deep-ultraviolet wavelengths of 0.125 µm to medium infrared wavelengths of 12 µm. As compared to other optical materials such as magnesium fluoride (MgF_2) and fused silica (SiO_2), CaF_2 is a relatively soft material in comparison to other optical materials. However, the low material fracture toughness classifies the ionic crystal as a brittle material.

Single-point diamond turning serves as an excellent solution to microfabrication of CaF_2 optics with intricate micro-features at high material removal rates. However, the material removal rate is limited by the brittle nature of the material that leads to micro-crack formation on the machined surfaces, a.k.a. brittle-mode machining. The micro-cutting process of crack-free surfaces is defined as ductile-mode machining, which is governed by a ductile–brittle transition (DBT) factor that commonly corresponds to a critical uncut chip thickness during micromachining [1]. The varying DBT values with respect to the crystallographic orientations add on to the difficulties of machining these optics [2]. Therefore, it is of crucial importance to investigate techniques that improve the machinability of the brittle material.

Several advanced machining technologies have been introduced to improve the machinability of CaF_2 such as ultrasonic vibration-assisted machining [3] and thermally-assisted machining [4–6]. Recently, Lee et al. [7] proposed an innovative and inexpensive method to increase the DBT during micro-cutting of CaF_2 with the use of an ink coating applied on the sample surface prior to micromachining. In addition to the improved machining performance, transmission electron microscopy analysis revealed a reduction in subsurface damage in the machined surface. The phenomenon was ascribed to be correlated to the effects of machining under high hydrostatic pressure exerted in a pressurized chamber by Yoshino et al. [8]. It is presently believed that the two methodologies to promote ductile-mode machining are governed by the same mechanics of crack formation, where the stress intensity factor is reduced due to the counteracting compressive stresses. In this paper, the new technique will be investigated using epoxy as the coating material to evaluate its effectiveness and process limitations in augmenting the production of micro-features on CaF_2 single crystals.

2. Experiments

A 0.8-mm round-nosed single crystal diamond cutting tool was set at a -10° rake angle and fixed on a Toshiba ULG-100 ultra-precision diamond turning machine for all the experiments (Figure 1). 10×10×5 mm sized CaF_2 samples were secured onto the air bearing spindle with a vacuum chuck. Prior to micro-cutting tests and coating applications, the sample surface was trimmed by face turning to achieve a flat surface with perfect reference to the cutting tool tip. The face turning process parameters were set at 1,200 rpm spindle speed, 1.0 mm/min feed rate and 10 µm nominal depth of cut. Oil coolant was used during the trimming process to achieve better surface finishing. The surface roughness of the face-turned CaF_2 sample was measured to be 1.92 nm Ra using an atomic force microscope (AFM) as shown in Figure 1(b). Cutting forces were measured at a frequency of 10 kHz using a Kistler 9256C1 dynamometer.

2.1. Radial-plunge cutting

As a standard practice in evaluating the ductile–brittle transition (DBT) during ultraprecision machining of brittle single

crystal materials, orthogonal plunge-cutting was performed on the (100) plane. Plunge-cuts inclined at 0.038° were performed radially at 15° intervals with a speed of 50 mm/min. Oil coolant was omitted from all plunge-cut experiments. A set of 24 grooves were made with and without a 2-µm coating layer. The ductile–brittle transition (DBT) was determined using optical microscopic imaging of the taper-cut grooves at the point where micro-cracks began to appear. The detailed DBT evaluation procedure in relation to the critical uncut chip thickness was described in Ref. [7].

The epoxy coating was set by comingling the epoxy resin and an aliphatic amine as the curing agent with a 1:1 ratio for 1 minute followed by the application of a layer of epoxy onto the machined CaF_2 sample surface and left to cure under the ambient conditions for 30 minutes. To achieve a uniform thick solidified coating on the sample surface, the coated sample was diamond turned on the ultra-precision machining centre with a spindle speed of 500 rpm and feed rate of 20 mm/min. The nominal cutting depth was set according to the desired coating thickness by offsetting the corresponding tool-workpiece displacement. For example, the tool will be set at 2 µm away from the CaF_2 surface to achieve a coating thickness of 2 µm. Figure 1(c) displays the top-view optical image of the machined epoxy coating surface.

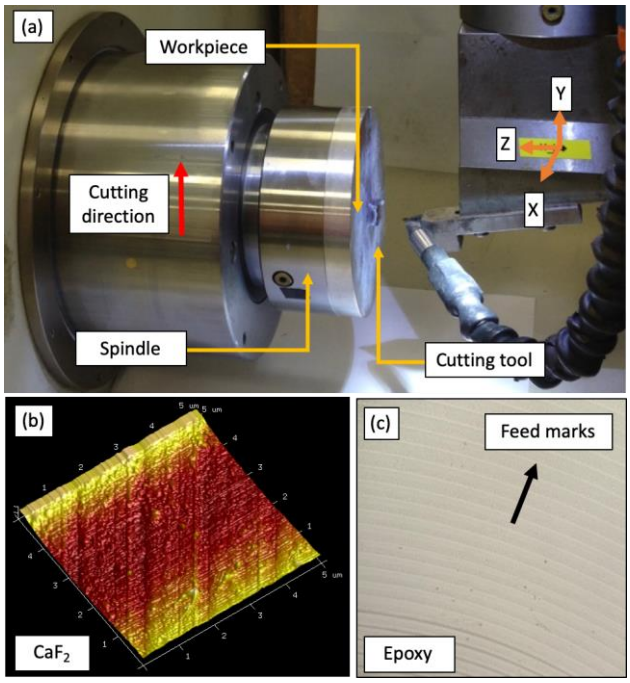

Figure 1. (a) Experimental setup on the ultra-precision machine center; (b) face-turned CaF_2 profile measurement by AFM; (c) optical image of the face-turned epoxy coating

In addition to the machining tests, a microhardness test was performed on the (111) plane using a Shimadzu HMV-2 Vickers microhardness tester to evaluate potential chemical effects during the application of the epoxy coating. Indentations were performed at 0.5 N with the indenter moving at 0.5 mm/s and dwelling in the material for 15 s. Three groups of indentations were performed – on an unaltered CaF_2 surface, a 10 µm coated surface, and a CaF_2 surface after the dissolution of the coating with ethanol. Indentation size effects [9] are negligible in this length scale.

2.2. Orthogonal plunge-cutting

To investigate the effectiveness of the coating on improving the DBT of CaF_2, orthogonal plunge-cuts were performed at an inclination angle of 0.014° to a final cutting depth of 2 µm. Plunge-cuts were performed along the $(111)[0\bar{1}1]$ direction over a total cutting length of 8 mm under dry cutting conditions at varying cutting speeds (100–400 mm/min). A set of grooves were first made without the solidified coating to define reference values for further comparison. Three plunge-cuts were performed at each cutting speed to decide the average DBT for each cutting condition.

Four variations of coating thickness were tested (2–10 µm) to evaluate the optimal thickness for enhanced material plasticity during micro-cutting. Prior to the coating process, the CaF_2 sample surface was first prepared by face turning on the ultra-precision machining centre with the process parameters listed Section 2.1.

3. Results and discussion

3.1. Ductile–brittle transition

Figure 2 presents the critical uncut chip thickness for DBT of each taper groove performed along different cutting directions on the (100) plane. The 4-fold symmetry characteristic of the (100) plane is displayed with the $[0\bar{1}1]$ direction showing the highest DBT depth of an average of 0.605 µm (without epoxy) along G1, G7, G13, and G19. In comparison, the average DBT depth with epoxy was enhanced by 126.1% to 0.763 µm. These results successfully demonstrate the use of the epoxy as a coating material to enhance ductile-mode machining with respect to different crystal orientations in comparison to the improvements observed by Lee et al. [7] in the use of solidified ink on the (111) plane.

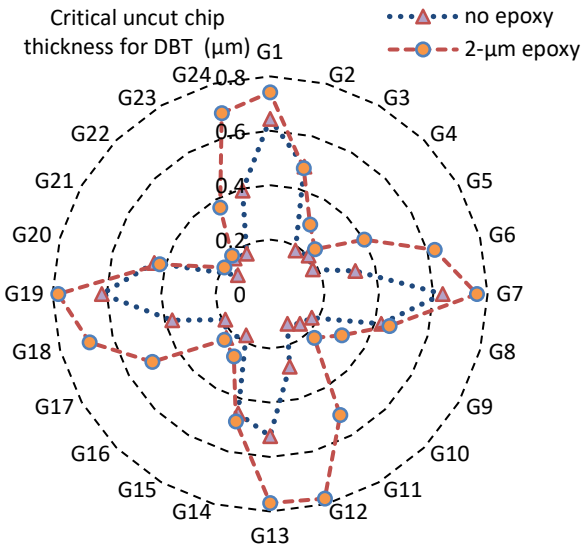

Figure 2. Critical uncut chip thickness along different cutting directions with and without epoxy coating and the first groove (G1) indexed along $(100)[0\bar{1}1]$

Vickers micro-hardness indentations before and after dissolution of the epoxy coating with ethanol showed negligible change in micro-hardness at 182.8 $HV_{0.05}$ and 182.0 $HV_{0.05}$, respectively. The indifference indicated insignificant chemical reactions between the coating and CaF_2. Therefore, the enhanced plasticity is justifiably ascribed to the mechanical influence of the coating. The microhardness of the epoxy was measured to be a tenth of that with CaF_2 at 19.98 $HV_{0.05}$, which provides further insights into the use of a relatively soft coating for effective enhancement in material plasticity during machining. The coating ductility is necessary for the coating to remain adhered to the workpiece surface during machining and to induce the necessary compressive stress. This suggests that there must exist a critical relationship between the mechanical

properties and thickness of the coating. On one hand, the use of a harder coating may possess stronger mechanical properties and correspondingly require a thinner coating thickness to provide the necessary compressive stresses. On the other hand, a super hard coating may exhibit certain degrees of brittleness that may lead to failure of the coating during machining and rendering the technique ineffective to enhance ductile-mode cutting.

The DBT depth shown in Figure 2 consistently increases with the use of the coating across all cutting directions. However, the magnitude of improvement is not a constant across all cutting directions such as the $[001]$ direction (G4, G10, G16, G24). The anisotropic DBT is strongly influenced by the Schmid factor, such that the plastic deformation will occur when the stress state exceeds the critical resolved shear stresses for slip deformation before surpassing the resolved tensile stress for cleavage fracture. In this aspect, the increased compressive stresses induced by the coating may be insufficient to suppress the cleavage stresses during cutting along certain directions. An increase in coating thickness may provide the enriched compressive stresses necessary to suppress crack formation during cutting. To this end, the effect of coating thickness is discussed in the subsequent section.

3.2. Influence of coating thickness

The critical uncut chip thickness results along the $(111)[0\bar{1}1]$ crystallographic direction with increasing coating thickness is reflected in Figure 3. The average improvement in DBT across the four cutting speeds with an 8 µm thick coating is 257.05% (i.e. an improvement factor of 2.57). The results are in good agreement with previous work performed on solidified ink in Ref. [7] where the DBT is governed by the coating thickness. It is important to note that the discrepancies in the reported critical uncut chip thickness when comparing with previous results [2,7,10] could be attributed to the differences in groove gradient, tool rake angle, and machine tool. Although the influence of the cutting speed cannot be clearly distinguished, an increasing DBT trend can be immediately observed with thicker coatings. Interestingly, there exists a maximum coating thickness of 8 µm before a decline in the critical uncut chip thickness.

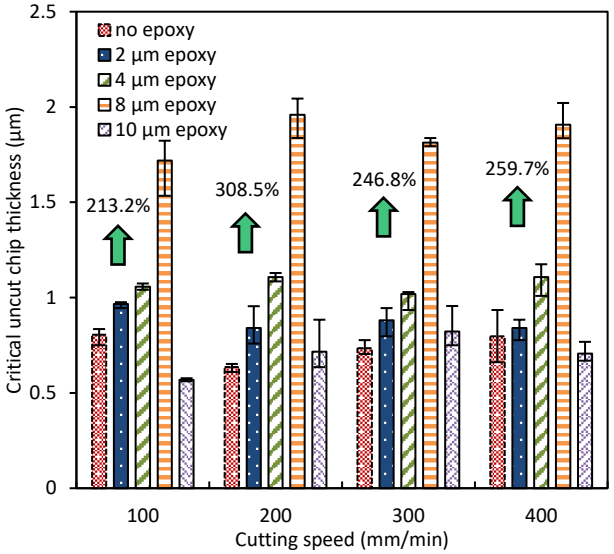

Figure 3. Critical uncut chip thickness in micro-plunge cutting of CaF_2 along the $(111)[0\bar{1}1]$ direction with increasing coating thickness and varying cutting speeds

The improvement in DBT depth can be associated with the resistance to deformation of the coating during machining, which induces compressive stresses into the work material ahead of the cutting tool to stabilize the cutting process. An infinitesimal element in the work material (Figure 4) can be used to study the stress state during cutting with the coating. The effective stresses acting on the work material can be estimated based on the tool-workpiece contact geometry and the machining forces. The tool exerts cutting forces (F_c) parallel to the cutting direction and thrust forces (F_t) perpendicular to the cutting plane. The effective areas (A_1, A_2) perpendicular to these respective forces shown in Figure 5 can be determined by Equations 1–5 that have been adapted from Ref. [11].

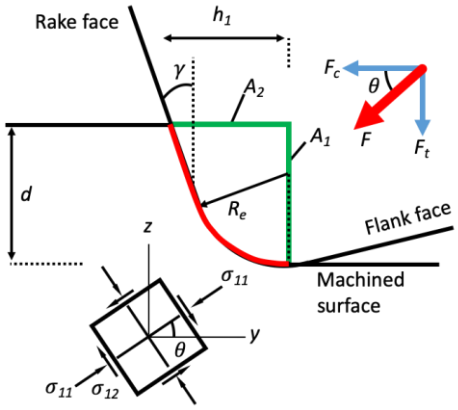

Figure 4. Schematic of stress status in an infinitesimal element during cutting

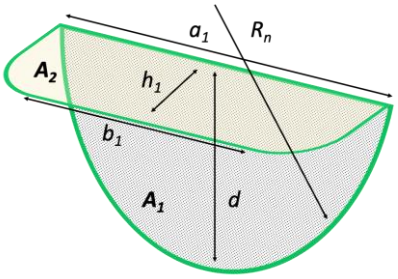

Figure 5. Effective tool-workpiece contact areas: (a) perpendicular to the cutting direction; (b) perpendicular to the cutting plane

$$h_1 = \tan\gamma\,[d - R_e(1 - \sin\gamma)] + R_e \quad (1)$$

$$a_1 = 2\sqrt{R_n^2 - (R_n - d)^2} \quad (2)$$

$$b_1 = \frac{2}{\cos\gamma}\sqrt{2R_n\cos\gamma\,(d - h_1\cos\gamma) - (d - h_1\cos\gamma)^2} \quad (3)$$

$$A_1 = \pi d\sqrt{R_n^2 - (R_n - d)^2} \quad (4)$$

$$A_2 = h_1 b_1 + \frac{1}{4}\pi h_1(a_1 - b_1) \quad (5)$$

where R_e and R_n are the tool edge radius and nose radius. γ is the tool rake angle and d is the effective cutting depth.

The stresses induced during cutting at the DBT can then be derived from the forces and the effective tool-workpiece contact areas in Equations 6 and 7. The principle stresses can then be resolved in Equations 8 and 9 where the angle θ can be determined from the ratio of the machining forces (Equation 10).

$$\sigma_y = \frac{F_c}{A_1} \quad (6)$$

$$\sigma_z = \frac{F_t}{A_2} \quad (7)$$

$$\sigma_{11} = \frac{\sigma_y+\sigma_z}{2} + \frac{\sigma_y-\sigma_z}{2}\cos 2\theta \quad (8)$$

$$\sigma_{12} = -\left(\frac{\sigma_y-\sigma_z}{2}\right)\sin 2\theta \quad (9)$$

$$\theta = \tan^{-1}\left(\frac{F_t}{F_c}\right) \quad (10)$$

Figure 6 presents the calculated normal stress (σ_{11}) and shear stress (σ_{12}) acting on the element based on the measured machining forces at the DBT of each plunge-cut along the $(111)[0\bar{1}1]$ direction. In general, a gradual increase in compressive and shear stresses with increasing coating thickness can be observed. The trend is in good agreement with the DBT results, where the workpiece sustains higher compressive forces prior to the activation of cleavage failure. The enhanced compressive forces tend to close and delay microcrack propagation by decreasing the tensile stress and the corresponding stress intensity factor [8]. The similar trend of increasing shear stress corresponds to the increase in shear strength of the workpiece as the material undergoes hydrostatic compression [12].

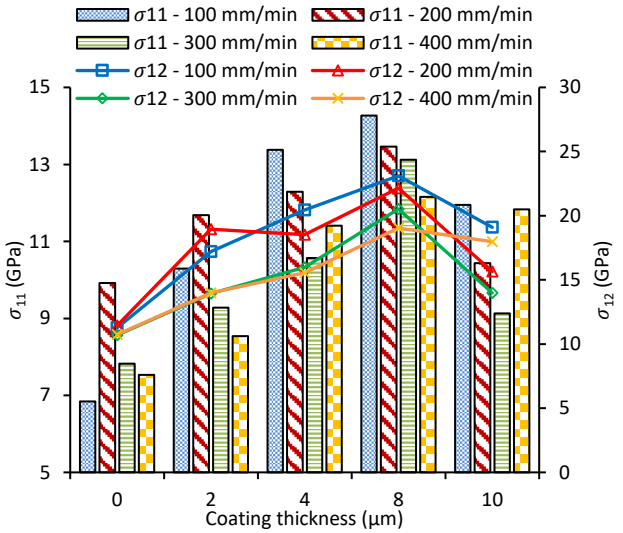

Figure 6. Calculated normal and shear stresses during cutting at the DBT zone with varying coating thickness and cutting speed

Interestingly, the further increase in coating thickness to 10 µm results is not effective for ductile-mode machining. This may imply that the excess pressure hinders the cutting efficiency as observed by Zhang et al. [13] in blowing high pressure air at the cutting zone. However, the decrease in compressive stresses indicates that the poor machinability is not caused by the excessive pressure on the work material but rather suggests that it was the detachment of the coating from the work material by either failure or loss of adhesion. According to Figure 3, there are instances where the DBT is relatively higher than conventional conditions and also negative effects. While the coating may have been dislodged from the work material surface, there still remains an opportunity for the broken coating to act as an obstacle in the machining path to provide the minute compressive stresses to enhance ductile-mode machining. On the other hand, the sudden failure or dislodging of the coating may cause an abrupt change in stress status of the work material that effects a large strain gradient that is known to affect the degree of plastic deformation. In this aspect, the coating material properties should also be considered for optimization of this methodology, where other machining parameters such as cutting speed will influence the machinability of the coating material. Moreover, precision control of the machining tool path can be explored to minimize machining time [14] and enable diamond shaping of microchannels [15].

The mechanics of the increase in pressure induced by the coating is analogous to the modified tool proposed by Uezaki et al. [16] where an additional jig is affixed a distance ahead of the cutting tool to exert compressive stresses on the work material during chip formation. However, the coating methodology dismisses the need for complex machine tools. At present, the current machining efficiency is hindered by the time required for coating solidification. Liquid resins that can rapidly solidify under UV exposure in milliseconds can potentially overcome this prevalent issue to make way for the fabrication of microfeatures with optical-grade quality.

4. Summary and future works

Ductile-mode machining of calcium fluoride (CaF_2) single crystals can be enhanced by applying solidified two-part type epoxy resin on the pre-machined surface. In this work, the ductile-brittle transition is augmented by an average magnitude of 2.57 during microcutting with a coating thickness of 8 µm. Fundamental estimations of the stress status of the work material suggests that there is an increase in compressive stress, which depends on the coating thickness. However, a limit to the coating thickness has been identified that may be a result of coating detachment from the work material. Future research will include the development of a micro-coating device using UV cured liquid resin to enable simultaneous coating and cutting.

Acknowledgements

The authors express their gratitude toward the financial support from Singapore Ministry of Education Academic Research Fund Tier 1 (Grant No.: R-265-000-593-114), and AcRF Tier 2 Funding (Project No.: MOE2018-T2-1-140). The authors would also like to thank Dr Hao Wang for his guidance in the research and Ms Jing Yi Chong for her assistance in the experimental work.

References

[1] Liu K, Wang H and Zhang X 2020 *Ductile Mode Cutting of Brittle Mater., Springer Nature Singapore*, 1-16

[2] Wang H, Riemer O, Rickens K and Brinksmeier E 2016 *Scr Mater* **114** 21-6

[3] Suzuki N, Nakamura A, Shamoto E, Harada K, Matsuo M and Osada M 2004 *Micro-Nanomechatronics Hum. Sci. 113-8*

[4] Shahinian H, Navare J, Zaytsev D, Kode S and Azimi F 2018 in: *33rd Annu. Meet. Am. Soc. Precis. Eng. Las Vegas, Nevada* 1-5

[5] Chaudhari A, Lee Y J, Wang H and Kumar A S 2017 in: *17th Int. Conf. Eur. Soc. Precis. Eng. Nanotechnol. (Euspen), 2017*

[6] Wang H, Kumar A S and Riemer O 2018 *Proc. Inst. Mech. Eng. Part B J. Eng. Manuf.* **232** 1123-9

[7] Lee Y J, Chong J Y, Chaudhari A and Wang H 2019 *Int. J. Precis. Eng. Manuf. Technol.* 1-11

[8] Yoshino M, Ogawa Y and Aravindan S 2005 *J. Mater. Sci. Eng.* **127** 837-45

[9] Chua J, Zhang R, Chaudhari A, Vachhani S K, Kumar A S, Tu Q and Wang H 2019 *Int. J. Mech. Sci.* **159** 459-66

[10] Mizumoto Y and Kakinuma Y 2018 *Precis. Eng.* **53** 9-16

[11] Yan J, Asami T, Harada H and Kuriyagawa T 2009 *Precis. Eng.* **33** 378-86

[12] Brinksmeier E, Mutlugünes Y, Klocke F, Aurich J C, Shore P and Ohmori H 2010 *CIRP Ann.* **59** 652-71

[13] Zhang X, Hui D, Liu K, and Wang H 2017 in: *17th Int. Conf. Eur. Soc. Precis. Eng. Nanotechnol. (Euspen), 2017*

[14] Vavruska P, Zeman P and Stejskal M *Procedia. CIRP* **77** 578-81

[15] Tan N Y J, Zhang, X, Neo, D W K, Liu K and Kumar A S 2019 in: *19th Int. Conf. Eur. Soc. Precis. Eng. Nanotechnol. (Euspen), 2019*

[16] Uezaki K, Shimizu J and Zhou L 2014 *Precis. Eng.* **38** 371-8